

GEODYNAMICS

Research within the Geodynamics Group of RSES covers three areas: (i) precise geodetic monitoring, modelling and analysis of crustal motion and deformation, (ii) glacial rebound and sea-level change and (iii) modelling of tectonic processes, including surface processes.

In the area of crustal motion and deformation research using geodetic methods the principal outcomes have been in two areas: the construction of a stand-alone Antarctic-conditioned GPS capability, powered by a combination of solar cell and hydrogen fuel cell technologies and with data transmission back to Canberra. At years end two packages are *en-route* to Antarctica for installation at Davis and Beaver Lake. This development follows on from very successful experiments in the previous two years with solar powered systems for day-light conditions. Two additional solar powered packages are also *en-route*, one for installation in the Southern Prince Charles Mountains and the other on the Prydz Bay coast. The purpose of the experiment is to measure differential vertical displacements between coastal and inland sites that may result from ice withdrawal from the Lambert Glacier drainage basin. The other major crustal displacement research has been the on-going Global Positioning System (GPS) surveys in Papua New Guinea with the survey of a detailed network in New Britain and New Ireland and a very recent survey in the northwestern region. With the principal first-order features of the plate tectonics of the region now defined with the GPS surveys, attention is now focussing on the details of the deformation across the boundaries. An important aspect of this work is the very close successful cooperation established with the National Mapping Bureau of Papua New Guinea, the Papua New Guinea National University of Technology at Lae, and the Rabaul Volcano Observatory.

In the area of glacial rebound, the work continues to focus on (i) new observational evidence from critical areas and times, such as north western Australia during the Last Glacial Maximum and the Ross Coast of Antarctica, (ii) the inference of ice sheet dimensions during the deglaciation phase from the sea-level data of Europe, and (iii) the inference of mantle rheology from the same data. Particular attention is placed on whether an effective separation of ice-and earth-model parameters can be achieved and the new inverse methods developed suggest that this is the case.

The third area of research is in lithospheric and crustal tectonic modelling which includes studies of the deformation of the Australian continent in early Palaeozoic time and more localized deformation in accretionary wedges and thrust belts. The numerical methods developed initially for these lithosphere-scale problems have also proved to be most applicable and efficient for studying surface processes and is leading to new insights into matters as diverse as glacio-fluvial erosion and karst aquifer evolution.

Dr Y. Yokoyama successfully defended his thesis this year and will join the Lawrence Livermore Laboratory, Berkeley, early in 2000. Ms E.-K. Potter joined the group as a PhD student. Two exchange students Ms S. Frederiksen and Mr Y. van Brabant, respectively from the Universities of Åarhus and Liège, joined the group for part of this year. Dr G. Kaufmann leaves the group to move to the University of Göttingen.

GEODETIC MONITORING OF MOVEMENTS AND DEFORMATION OF THE CRUST

Papua New Guinea

P. Tregoning, H. McQueen, K. Lambeck, R. Jackson¹ and R. Little¹

In 1999 the RSES equipment which is on long-term loan to the University of Technology, Lae, was used by staff and students at that University, and on our behalf, to make repeat observations at key sites on the Huon Peninsula in and around the Ramu-Markham Fault zone and observations were made at Wewak by a student from RSES. We also supported staff at the Rabaul Volcano Observatory in their monitoring of active volcanoes in the New Britain/New Ireland region by supplying GPS equipment for fieldwork and by analysing the data and providing up-to-date coordinates of the sites monitored.

In addition, several sites in the northwestern region of Papua New Guinea were observed in late November at sites first observed with GPS in 1993. These data have allowed crustal velocities to be estimated at sites surrounding the location of the July 1998 earthquake and tsunami, which devastated the northern coastline near Aitape. The new information is leading to a better definition of the kinematics of this region and, ultimately, to the tectonic forces responsible.

On 1 April, 1999, a $M_w=6.2$ earthquake occurred on the Weitin Fault, New Ireland. The earthquake location is within the GPS network observed by RSES and Unitech in September 1998. At our request, staff and students at Unitech organised and executed a repeat survey at the four sites closest to the epicentre of the earthquake. Analysis of the data is underway; preliminary estimates indicate that the earthquake caused less than 20 mm displacement at the GPS monitoring sites. This highlights the need for long-term station occupation in order to separate inter- and co-seismic deformation on and adjacent to the faults.

The data collected in the New Ireland and New Britain regions in 1998 have been combined with other GPS and terrestrial geodetic data observed since 1975 to estimate a preliminary velocity field for the Gazelle Peninsula and southern New Ireland. The pattern of individual site velocities with respect to the South Bismarck Plate reveals a relatively uniform velocity gradient across a 150 km region between the rigid South Bismarck and Pacific Plates, indicative of a locked strike-slip boundary (Figure 1). Anomalous velocities at two sites on the west coast of New Ireland indicate that a $M_w=7.1$ earthquake in 1985 may have caused co-seismic deformation between the 1975 terrestrial survey and 1994–1998 GPS surveys.

We have developed a DOS-based computer program that synthesizes the current understanding of present-day tectonic motion to allow users to estimate the velocity of a site anywhere in Papua New Guinea. From input coordinates of the site(s), the program calculates on which plate the site resides, the site velocity and the site coordinates at any other epoch. It also allows users to calculate the distance (and rate of change of distance) between any two points, and to calculate the coordinates of new sites while accounting for the effects of tectonic motion. The program has been provided to the Papua New Guinea National Mapping Bureau and interested university groups within Papua New Guinea to provide them with a tool for accounting for the active tectonic environment in their geodetic measurements.

¹ Department of Surveying and Land Studies, The Papua New Guinea University of Technology, Lae

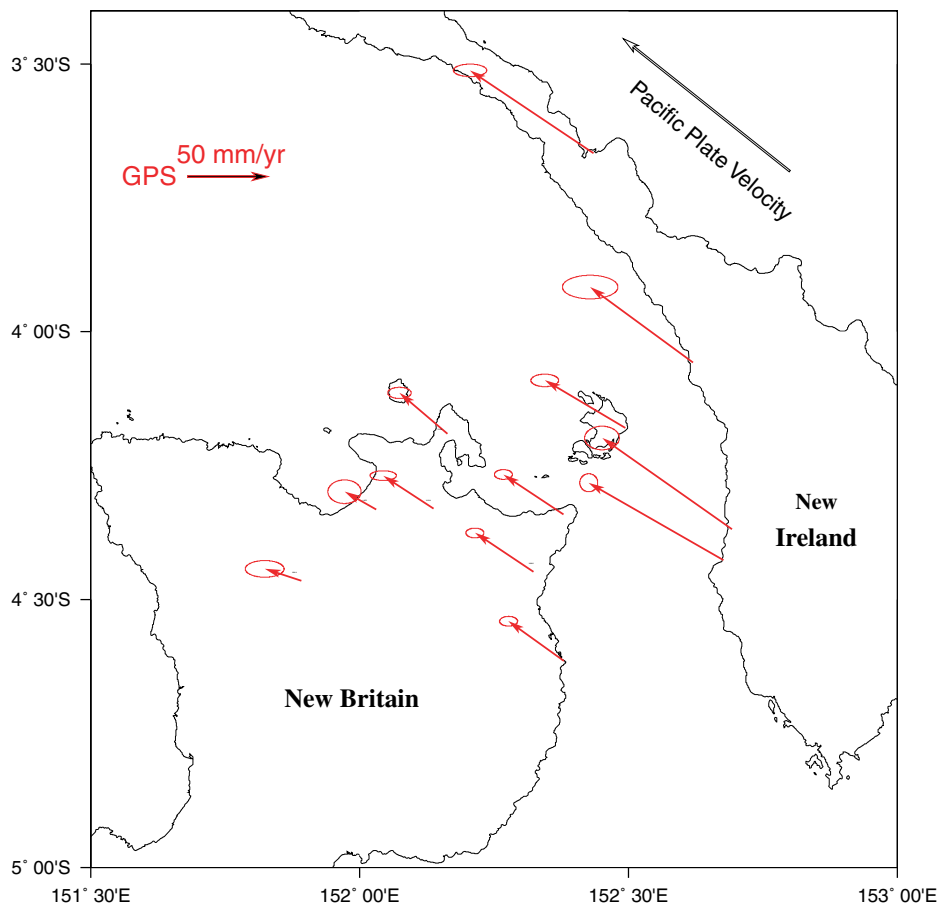


Figure 1: GPS site velocities relative to the South Bismarck Plate. The relative motion of the rigid Pacific Plate is indicated with a white arrow.

Antarctica - Isostatic Rebound

P. Tregoning, H. McQueen, A. Welsh, N. Schram and K. Lambeck

In January 1999, the equipment installed at Beaver Lake, Antarctica in January 1998 was revisited and found to have survived the winter intact. Ten weeks of GPS data were recovered, along with diagnostic data which showed that the solar-powered system operated until 26 March by which time solar energy was insufficient to power the system. This was a major achievement since other international groups attempting to operate remote GPS installations are suffering from major equipment failures whereas our simple, solar-powered system operated as expected. A new set of six solar panels have been installed, along with a new GPS receiver. Ten days of data were recovered before the system was left unattended for the rest of the year. It will be revisited in January 2000, at which time we expect to recover additional data observed in February/March 1999.

There is currently no proven means of providing significant power to remote equipment throughout an Antarctic winter, and during 1999, a major new initiative was undertaken to enhance the equipment for the remote GPS installations in Antarctica. A 1998 ANU Major Equipment proposal to purchase hydrogen fuel cells (manufactured by Hydrogenics Corporation) and a Satcom-B satellite phone was successful and these items were purchased this year. The fuel cells combine hydrogen gas with oxygen from the surrounding air to generate electricity, heat and water. The electricity supplies the power to operate the equipment during the winter periods of darkness when there is insufficient solar power available. This will be the first

time that fuel cells have been used to provide power to remote equipment in Antarctica and will represent a significant scientific breakthrough if successful.

The RSES Electronics Group designed and built power controllers, computers and power switching devices to integrate the solar and fuel power and to provide power to peripheral equipment when required. The power controller runs continuously (consuming ~ 0.8 W) and constantly monitors the battery voltages and the internal temperature of the equipment housing. Diagnostic data is logged, including information about the performance of the fuel cell, and is transferred to the computer each day. Once per day, the computer is powered up (2.5 W) to download the data from the GPS receiver, to convert it to a more compact format, collect the diagnostic data from the power controller, and transmit all the data back to RSES via satellite phone.

Equipment housings and mounting structures are shown in Figures 2 and 3. All equipment is raised above the ground to prevent snow drifts forming on the leeward side of the structures. The insulation of the equipment was designed to be a passive system without the need for venting or any active, moving components. Knowledge of the expected temperature ranges and changing power usage inside the equipment housing has been used to create an enclosure that will maintain an internal temperature of between 5° and 50°C. In the event that the outside temperature falls below -40°C, heaters will automatically switch on inside the enclosure to ensure that the inside temperature remains above 5°C; otherwise, the heat of the operating equipment will be sufficient to keep itself warm.

The equipment will be installed at Beaver Lake in January 2000 and it is expected to operate throughout the whole of the year. A similar system will be operated at Davis, where the performance of the fuel cell can be monitored directly to provide feedback on how the Antarctic environment affects the operation (eg icing up of the exhaust outlet, rate of hydrogen consumption). In addition, two new solar-powered sites will be installed in January in the Lambert Glacier region as part of a long-term expansion of the GPS network.

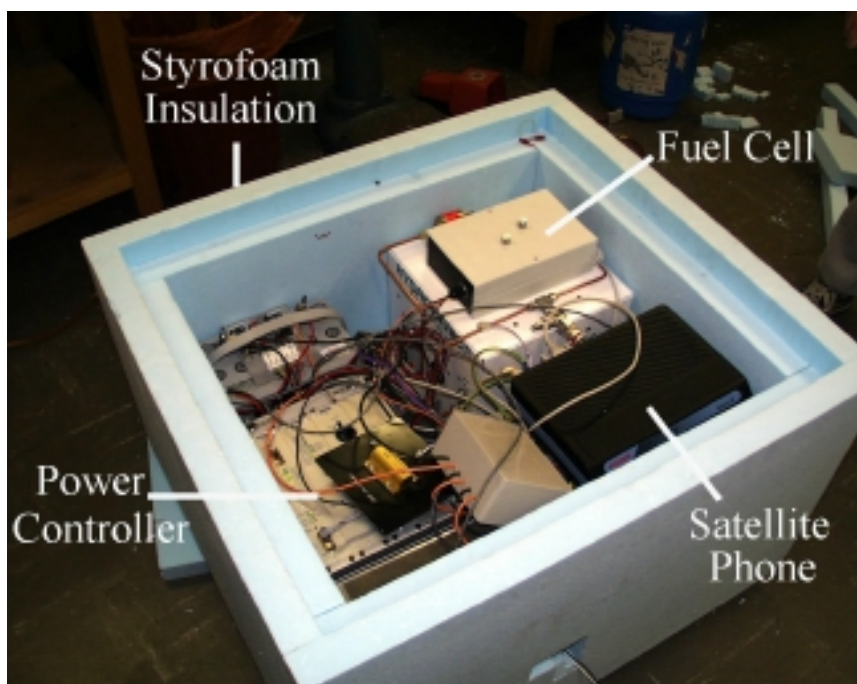


Figure 2: Power controller, fuel cell, satellite phone and associated electronics developed at RSES for the remote Antarctic GPS installations.



Figure 3: Part of the equipment setup to be deployed at Beaver Lake and Davis in January 2000. The satellite phone radome can be seen on the left. An additional set of three solar panels will be installed further to the left of the radome, resulting in six panels to generate solar power at each site.

Super-Gravimetry

H. McQueen , K. Lambeck and T. Sato²

Mt Stromlo Gravity Station continues to operate successfully and is proving to be one of the most sensitive of the worldwide Superconducting Gravimeter (SG) sites. A major calibration with an FG5 Absolute Gravimeter was performed at the station in February during a visit by Dr Amalvict from EOST at the Université Louis Pasteur in Strasbourg with support from AUSLIG. These determinations provide the necessary calibration of the superconducting instrument and permit the measurement of its drift characteristics and the secular change of gravity at the site, which is essential for analysis of long period processes.

The SG is currently the most sensitive type of gravity meter, built around a superconducting niobium sphere levitated by a magnetic field in an evacuated chamber and cooled by a liquid Helium bath. Gravity fluctuations down to one part in 10^{12} of earth's surface gravity can be determined by accurate monitoring of the sphere's position. Operation of the Canberra site is a collaboration between the Geodynamics group in RSES and the Japanese National Astronomical Observatory, Mizusawa, and data is regularly archived at the data centre of the Global Geodynamics Project. It is part of a world-wide array making precise observations of faint gravity signals in an attempt to detect motions in the deep interior, infer details of Earth's internal structure, and provide information on a range of problems in global geodynamics.

The Canberra site is one of the few at which background free oscillations of the Earth, apparently unrelated to major earthquake excitation, have recently been observed. These faint oscillations constitute a steady hum of subtle vibrations of the whole earth whose source has not yet been definitely identified. The main suspect at this stage is excitation by atmospheric pressure fluctuations but longer and more sensitive records at several sites are needed to test this hypothesis. Because of its sensitivity, the Canberra site will provide one of the most important records in this study.

² National Astronomical Observatory of Japan, Mizusawa

ICE SHEETS, SEA LEVEL AND MANTLE VISCOSITY

Sea-level constraints on the termination of Last Glacial Maximum and global ice volume variations

Y. Yokoyama, K. Lambeck, P. De Deckker³, P. Johnston, L.K. Fifield⁴, A. Purcell

New sea-level observations from the Bonaparte Gulf in north western Australia constrain the magnitude and rates of change of ice volumes during the Last Glacial Maximum (LGM) and early period of the Late Glacial stage. The region is tectonically stable and far from the former ice-covered regions. The glacio-hydro-isostatic adjustment of the coast is relatively small and the corrections for this effect are not sensitive to details of the rebound model. Microfossil analysis and AMS radiocarbon dating of a number of cores taken across the shelf and Bonaparte Gulf demonstrate that (i) the LGM sea-levels were locally at -125 ± 4 m, (ii) the LGM terminated abruptly at 19,000 cal yr BP with a rapid rise in sea-level of about 15 m over the next 500 years, (iii) the onset of the minimum sea-levels occurred before 22,000 cal yr BP. When corrected for the glacio-hydro-isostatic effects, the increase of LGM ice volumes over present day ice volume is 52.5×10^6 km³. The termination of the LGM is marked by a rapid ice discharge of 5.2×10^6 km³.

Sea-level change along the French Mediterranean coast for the past 30 000 years

K. Lambeck, E. Bard⁵ and A. Purcell

Observational evidence for sea-level change along the French-Mediterranean coast has been examined and compared with glacio-hydro-isostatic models to predict the spatial and temporal patterns of change for about the past 30,000 ¹⁴C years. These predictions are pertinent to discussions of changing ocean volumes during this interval, the tectonic stability or otherwise of the coastal areas, mantle rheology, and the timing of possible human occupation of the now-submerged coastal plain and caves, such as Cosquer Cave near Marseille. The principal results from the analysis are: (i) Sea levels along this section of the coast have risen continually since the time of the Last Glacial Maximum (LGM) and at no time during the Holocene has mean-sea-level been higher than that of today. (ii) The coast has been tectonically stable between Marseille and Nice as well as further to the west in Roussillon. Western Corsica may have experienced a slow tectonic uplift of between 0.15 to 0.3 mm/year for the past 3000 years but northernmost Corsica appears to have been stable during this same interval. (iii) During the LGM sea levels along the coast and immediate off-shore areas stood at between 105–115 m below present level, the range reflecting the importance of the isostatic contributions. During oxygen isotope stage 3 sea levels do not appear to have risen locally above about -60 m. (iv) The rebound parameters (describing the mantle rheology and ice sheets) required to match the limited observational evidence are consistent with the results of similar analyses carried out for other parts of Europe. Because of its distance from the former northern ice sheets the isostatic factors are particularly sensitive to the value of the lower mantle viscosity. (v) The model predictions for sea-level change at the Cosquer Cave site and for its immediate environments indicate that the cave was last readily accessible before about $10,700 \pm 500$ ¹⁴C years (about $12,500 \pm 500$ cal. years) BP and that the cave entrance was completely flooded by 9000 ± 200 radiocarbon years BP (between about 9800 and 10,300 calibrated years BP). The cave was above sea level throughout the oxygen isotope stage 3.

³ Department of Geology, ANU

⁴ Department of Nuclear Physics, RSPHYSSE, ANU

⁵ CEREGE, Université d'Aix-Marseille III, CNRS, France

Constraining late glacial ice in the Ross Embayment

J.M. Quinn, K. Lambeck and J.O. Stone⁶

A number of different dating methods have been applied to the isostatically-raised shorelines of McMurdo Sound, in the Ross Sea, Antarctica. AMS ¹⁴C dating of molluscs and penguin eggshell from within raised deltas and beaches have been combined with a recently published dataset to form a relative sea-level curve for the Scott Coast of McMurdo Sound. OSL dating in progress, is indicating a Holocene age for the same beaches and is in agreement with the radiocarbon dating.

Surface exposure dating of the beach boulders, bedrock platforms and boulder pavements using the isotope chlorine-36 has also been carried out. The results from this dating show an age progression with height from sea level but with a component of earlier exposure. These field results have been combined with forward modelling of the isostatic rebound of the coast in response to changes in ice loading, to determine possible end members of ice volumes for Antarctica in Late Glacial times, specifically in the Ross drainage basin. The starting point for these models has been to use a recognised maximum model (Denton and Hughes 1981) in which ice extends out to edge of the continental shelf, and a minimum model with less ice from Huybrechts. Modification of these two models for the Ross Embayment area predict relative sea-level curves for McMurdo Sound which are compared to the field results to develop a suite of possible ice models for the Ross drainage basin. Ice melting from the area of Antarctica outside of the Ross drainage basin has a minimal isostatic rebound effect in McMurdo Sound. The results show the importance of knowing the timing of melting as well as the regional ice volume. Sites at a distance from Antarctica can help constrain melting times. Using a melting scenario similar to the Northern Hemisphere ice sheets, only about 50% of the maximum model ice volume for the Ross drainage basin area is required.

Inference of ice sheet history

P. Johnston and K. Lambeck

Sea-level observations from sites close to the ice sheets of the last ice age contain information on the glacial history of these regions and the Earth's response to glacial loading. If the Earth's rheology is well known, the observations can be used to estimate the ice thickness through time. However, many different glaciation histories are capable of producing a given set of observations, so an extra criterion is required to select the best model from all possible models. Previously, the best fitting model has been selected from the population of adequately fitting models. But the best fitting model is usually unrealistically rough and introduces spurious details into the inferred model not warranted by the observations. Instead, we have developed a method of selecting the smoothest model which adequately fits the sea-level observations. Also, near the edge of large ice sheets, and for smaller ice sheets, some mountains protruded through the ice at the Last Glacial Maximum as nunataks. Trimlines marking the boundary between glaciated and unglaciated terrain can be observed in the field and their elevations are used as constraints on the maximum elevation of ice during the last ice age.

The above method has been applied to 441 sea-level observations from the British Isles dating back to 15,000 years ago. The extent and timing of the retreat of the British ice sheet was compiled from field data and digitised onto a 50 km grid at 1000 year intervals from 27 to 13 thousand years ago for a total of 2077 model parameters. The model with the smoothest elevation which fits the sea level data with a root mean square error of 1.3 and fits all of the trimline observations is shown in Figure 4. The ice heights are shown for every second time step and the maximum elevation of ice in Scotland is about 1500 m. The fact that a root mean square error of 1 is not possible with this earth model suggests that it may be possible to infer mantle viscosity with this method as well as the ice sheet history. Such an estimate would be

⁶ Department of Geological Sciences and Quaternary Research Center, University of Washington

more robust because it would not depend necessarily on the assumed ice distribution as is the case for previous inferences of earth rheology.

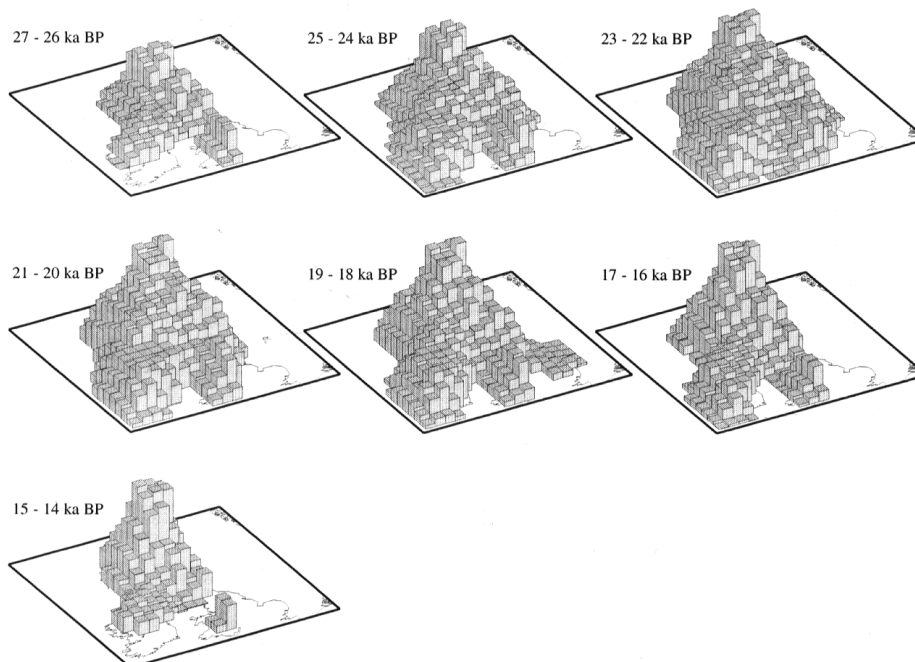


Figure 4: Minimum roughness ice elevation model inferred from sea level and ice elevation observations in the British Isles.

Mantle dynamics, postglacial rebound and the radial viscosity profile

G. Kaufmann and K. Lambeck

We infer the radial viscosity structure of the Earth's mantle from observations of the long-wavelength geoid and glacially-induced sea-level changes, changes in the Earth's rotation and gravitational field. We employ a combination of forward and formal inverse modelling of long-term mantle circulation driven by large-scale density differences deduced from seismic tomography. Based on the resulting unscaled mantle viscosity profiles, we model the time-dependent glacial isostatic adjustment of the Earth related to past and present changes in the ice-ocean mass balance and we deduce scaled mantle viscosity profiles, which simultaneously fit the long-wavelength geoid constraint and glacially-induced changes of the Earth's shape.

Two mantle viscosity profiles fit the observational data equally well (Figure 5). Both profiles are characterised by a two order of magnitude variation of viscosity within the Earth's mantle. Variations of viscosity in the upper mantle are less than one order of magnitude. In the lower mantle, the viscosity differs significantly with depth for both models. The first model is characterised by a rather smooth variation in viscosity across the 660 km seismic discontinuity, and viscosities increase towards the central parts of the lower mantle, then they decrease again towards the core-mantle boundary. Average viscosities in the upper and lower mantle are around 1×10^{21} and 3×10^{22} Pa s, respectively. In the second model viscosity jumps by two orders of magnitude across the 660 km seismic discontinuity, and peak values in the lower mantle occur around 1000 km depth. Below, viscosity decreases towards the central parts of the lower mantle, and increases again closer to the core-mantle boundary. Average viscosities in the upper and lower mantle are around 5×10^{20} and 8×10^{22} Pa s, respectively.

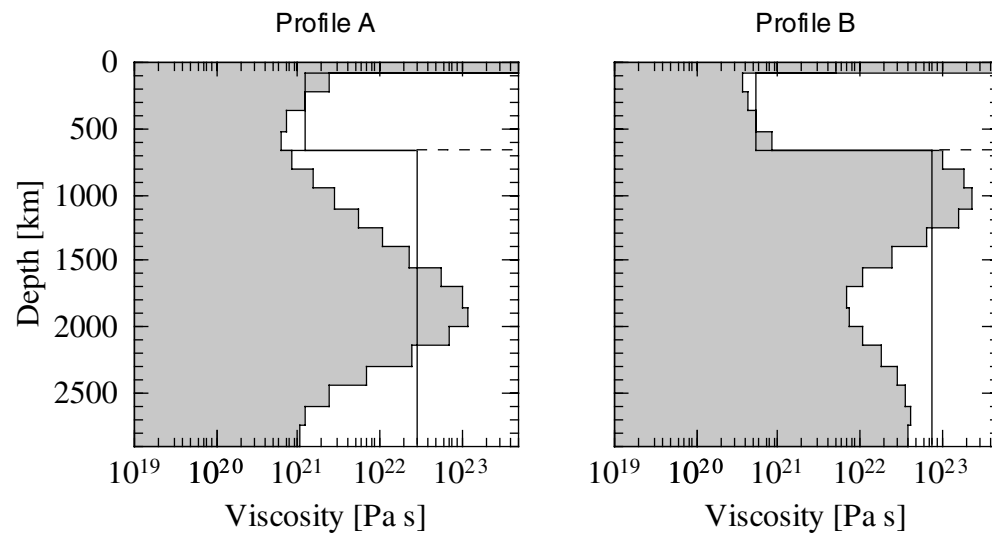


Figure 5: Preferred viscosity profiles derived from this study. The thick dashed lines indicate the volume-averaged upper- and lower-mantle viscosity values, the thin dashed lines represent the 660 km seismic discontinuity.

Glacial isostatic adjustment in Fennoscandia on a laterally heterogeneous Earth

G. Kaufmann, P. Wu⁷ and G. Li⁷

Glaciation and deglaciation in Fennoscandia during the last glacial cycles has significantly perturbed the Earth's equilibrium figure. Changes in the Earth's solid and geoidal surfaces due to external and internal mass redistributions are recorded in sequences of ancient coastlines, now either submerged or uplifted, and are still visible in observations of present-day motions of the surface and glacially-induced anomalies in the Earth's gravitational field. These observations become increasingly sophisticated with the availability of GPS measurements and new satellite-gravity missions.

Observational evidence of the mass changes are widely used to constrain the radial viscosity structure of the Earth's mantle. However, lateral changes in earth model properties are usually not taken into account, as most global models of glacial isostatic adjustment assume radial symmetry for the earth model. This simplifying assumption contrasts with seismological evidence of significant lateral variations in the Earth's crust and upper mantle throughout the Fennoscandian region. On the assumption that the short-term seismologically-inferred variations in Earth properties are at least in part related to long-term viscosity variations, we deduce a three-dimension viscosity structure for our model calculations.

We compare predictions of glacial isostatic adjustment based on a realistic ice model over the Fennoscandian region for the last glacial cycle for both radially symmetric and fully three-dimensional earth models. Our results clearly reveal the importance of lateral variations in lithospheric thickness and asthenospheric viscosity for glacially-induced model predictions. Relative sea-level predictions can differ up to 10–20 m, uplift rate predictions by 1–3 mm yr, and free-air gravity anomaly predictions by 2–4 mGal, when a realistic three-dimensional earth structure as proposed by seismic modelling is taken into account.

⁷ Department of Geology and Geophysics, University of Calgary, Canada

Last ice age millennial scale climate changes recorded in Huon Peninsula corals

Y. Yokoyama, T.M. Esat, K. Lambeck and L.K. Fifield⁴

Uranium series and radiocarbon ages have been measured in corals from the uplifted coral terraces of Huon Peninsula, Papua New Guinea, to provide a calibration for the radiocarbon time-scale for times older than 30,000 years BP (before present). Diagenetically altered samples were eliminated through improved analytical procedures and quantitative criteria for sample selection. The base-line of the calibration curve follows the trend of increasing divergence of the radiocarbon timescale from calendar ages established by previous studies. Superimposed to this trend are four well defined peaks of excess atmospheric radiocarbon level (>200% relative to current levels). These peaks correlate with the timing of specific periods of reef growth at Huon Peninsula and appear to be synchronous with Heinrich events and concentrations of ice-rafted debris found in North Atlantic deep sea cores. Timing of these phenomena suggests the following sequence of events: An initial sea-level high (interstadial period) is followed by a large increase in atmospheric radiocarbon as the sea-level falls during the next phase of ice growth. Over ≈1800 years the atmospheric radiocarbon drops to below present ambient levels. This cycle bears a close resemblance to ice-calving episodes of Dansgaard-Oeschger and Bond cycles and the slow-down or complete interruption of the North Atlantic thermohaline circulation. The increases in the atmospheric radiocarbon levels are attributed to the cessation of the North Atlantic circulation.

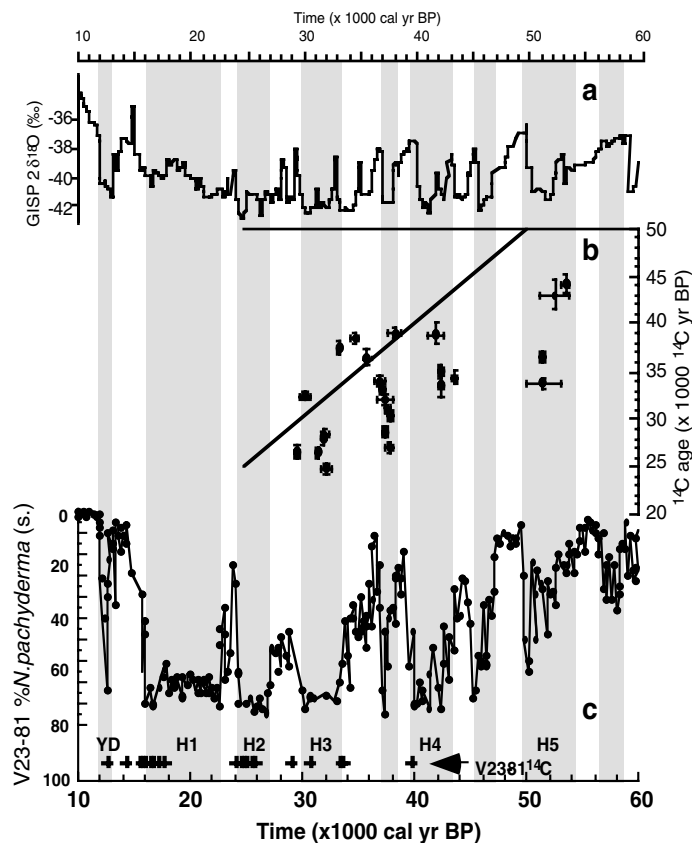


Figure 6: Four discrete $\Delta^{14}\text{C}$ peaks found in the present study (b) are coincident with Heinrich events (H) found in the North Atlantic Sea Surface temperature record (c: after Lund and Mix 1998) and temperature fluctuations appeared in the Greenland ice core record (a). U/Th dated $\Delta^{14}\text{C}$ peaks can defined exact timing of H3, H3.5, H4, and H5.

MODELLING OF TECTONIC PROCESSES AND LANDSCAPE EVOLUTION***The OZBLOCK project: a thin-plate model of Palaeozoic deformation of the Australian lithosphere.***

J. Braun and R.D. Shaw⁸

We have developed a thin-plate model of the continental lithosphere in which deformation is driven by in-plane forces originating along plate boundaries. The geometry of the model, the strength of each lithospheric block, and the boundary forces have been chosen to reproduce the major tectonic episodes experienced by the Australian continent during a 200 Myr time period starting in the Ordovician (ie 470 Ma). The model's focus is on the reactivation and/or reworking of zones of weakness within the continent that have either been set a priori or have developed in response to previous tectonic regimes.

The tectonic history of the Australian continent has been used as a natural laboratory to test hypotheses on the nature and style of intracratonic deformation. We demonstrated that intracratonic deformation (ie deformation that takes place away from active plate boundaries) results from the concentration of horizontal stress originating at plate boundaries into regions of decreased lithospheric strength; these weak zones are often caused by previous intracratonic deformation and/or develop at the interface between regions of contrasting strength. We also showed that repeated episodes of deformation may lead to strain localization. Concentration of strain in narrow corridors may also result from the constructive interaction between two sets of tectonic forces acting on separate margins. Our study also demonstrated that there are mechanisms that operate within the lithosphere (such as post-extensional mantle healing) by which deformation leads to local strengthening.

Numerical modelling of strain localisation in the mantle lithosphere

S. Frederiksen⁹, J. Braun and S.B. Nielsen¹

Deep seismic data from the Central Graben in the North Sea (see Figure 7) shows dipping reflectors in the upper mantle. It has been debated whether these features are traces from a subduction zone or shear zones developed during extension. Joint inversion of seismic (MONA LISA) and gravimetric data gives a good constrain on the outline of the basin and the crust beneath.

Using numerical models developed at RSES, we have shown that large-scale shear zones can develop in the mantle lithosphere when strain softening takes place during lithospheric extension and rifting. The development and geometry of the shear zones depends on the value of model parameters such as the assumed geothermal gradient, the rate of extension and the assumed pre-extension crustal thickness. Furthermore results show that the deformation pattern in the lithosphere can be strongly affected by the strength of the syn-extensional sediments.

⁸ Australian Geological Survey Organisation

⁹ Department of Geophysics, University of Aarhus, Denmark

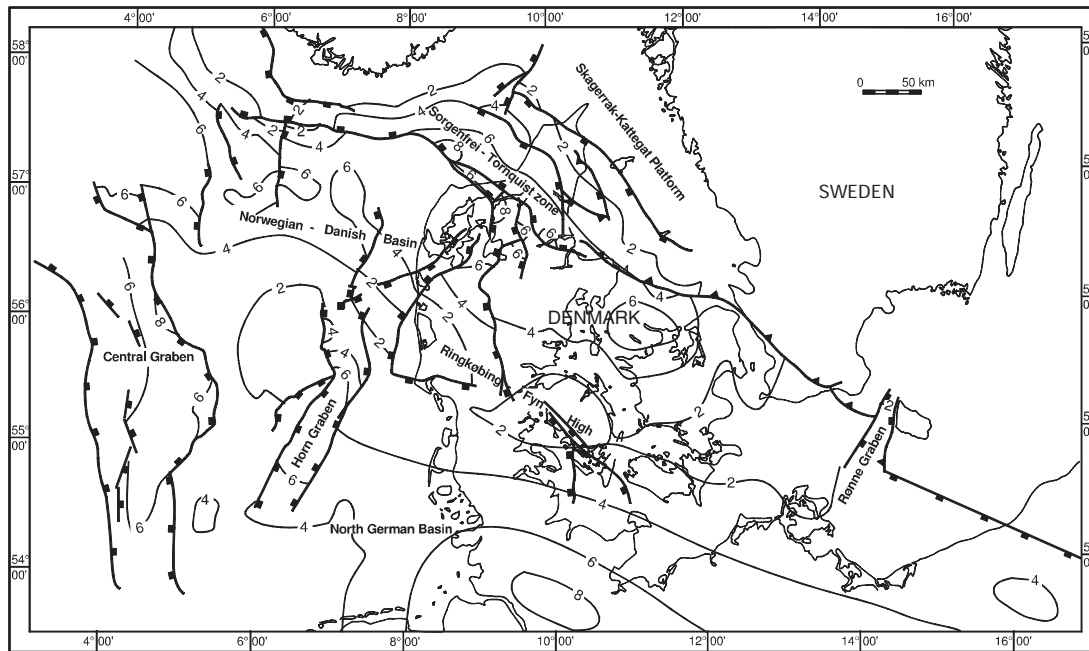


Figure 7: The main tectonic and structural features in the Danish and surrounding area. Isolines show the depth in kilometers to the pre-Zechstein surface.

Numerical models of faulting during crustal compression

D.R. Burbidge and J. Braun

The long-term evolution of the mechanical behaviour of the crust under compression (eg in accretionary wedges and fold-and-thrust belts) has always been difficult to model with traditional physical and numerical methods. This is primarily due to the large amounts of strain localization that characterizes the upper brittle crust (ie faulting). A new type of numerical method (the Distinct Element Crustal Model, or DECM) has been developed over the last few years which allows us to study problems involving substantial amounts of strain localization, even after large accumulated strain.

A large range of numerical experiments have been conducted to better understand the behaviour of brittle-frictional crustal material accreting against a rigid backstop. This could (for example) correspond to a sedimentary layer being accreted against stronger material (the continental basement) at a subduction zone. Two types of behaviour were observed, which depend mainly on the value of the basal friction coefficient. For low basal friction (eg a weak or wet base), the deformation occurs mainly by frontal accretion and the formation of so-called "pop-up structures" (Figure 8a). For high basal friction (strong base), the deformation is primarily accommodated by accretion near the back of the sedimentary pile following basal underthrusting under a flat-ramp fault (Figure 8b). At intermediate values of the basal friction, the behaviour of the accreting sedimentary wedge oscillates between these two modes (Figure 8c). Both end-member behaviours can be observed at subduction zones, and the oscillation between the two could explain observed changes in slope along the strike of some accretionary wedges (eg the Alaskan accretionary prism).

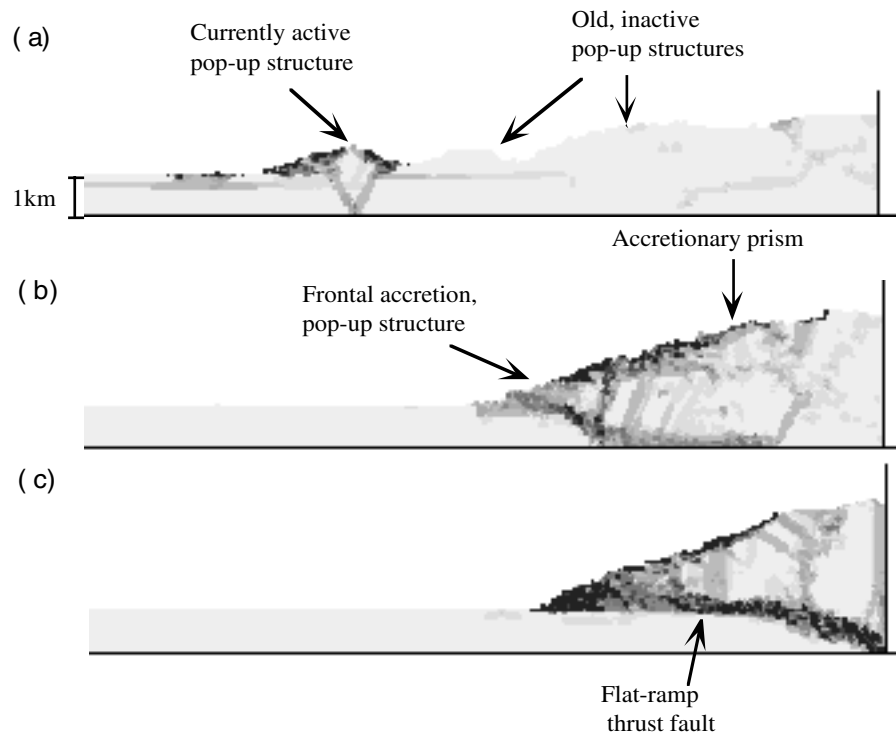


Figure 8: Three models illustrating the different faulting behaviour for three accretionary prisms with three different basal frictions: (a) low friction (basal co-efficient of friction (μ_b) of 0.2, (b) high basal friction ($\mu_b = 0.8$) and (c) intermediate basal friction ($\mu_b = 0.5$). All models have the same element-element friction of 0.5. (a) is dominated by frontal accretion and the formation of pop-up structures, while (c) is dominated by underthrusting and uplift near the rear of the prism. (b) oscillates between the two modes (it is pictured during a period of frontal accretion). During periods of frontal accretion (b) undergoes normal faulting near the top of the prism. Synorogenic extension like this has been observed at the top of some accretionary prisms (eg Taiwan).

Landforming processes in a tectonically active region: a glacio-fluvial erosion model of the Southern Alps, New Zealand

J.H. Tomkin and J. Braun

The Southern Alps of New Zealand is a zone of tectonic activity, caused by the collision between the Pacific and Australian plates. For the last few million years, convergence across the plate boundary has not led to substantial growth of the mountain belt, suggesting that, in the South Island of New Zealand, rock uplift is in equilibrium with surface erosion. Although present-day surface erosion is dominated by landsliding of over-steepened valley walls and transport of debris by fluvial transport, it is well documented that, during the last two million years, the Southern Alps were affected by glaciations during which glacial abrasion must have played an important role in setting the equilibrium between uplift and erosion.

Previous geochronological studies based on fission track, K-Ar and Ar-Ar dating of surface rocks from the region have led to the formulation of a range of scenarios to describe this equilibrium. The distribution, amount and rate of uplift along and across the strike of the orogen are still matters of debate. By using a surface processes model that incorporates fluvial, hillslope and glacial erosion, we are able to test the validity of proposed uplift regimes. We have simulated a variety of uplift scenarios and produced quantitative estimates of the resulting denudation for a range of parameters of our surface processes model. In particular, we tested the relative importance of each land-sculpting process, as well as the effect of the observed asymmetry in

precipitation. As an example, we show in Figure 9 the predicted topography from a model run at the peak of an assumed glacial maximum, with the overlying ice thickness denoted by the shading.

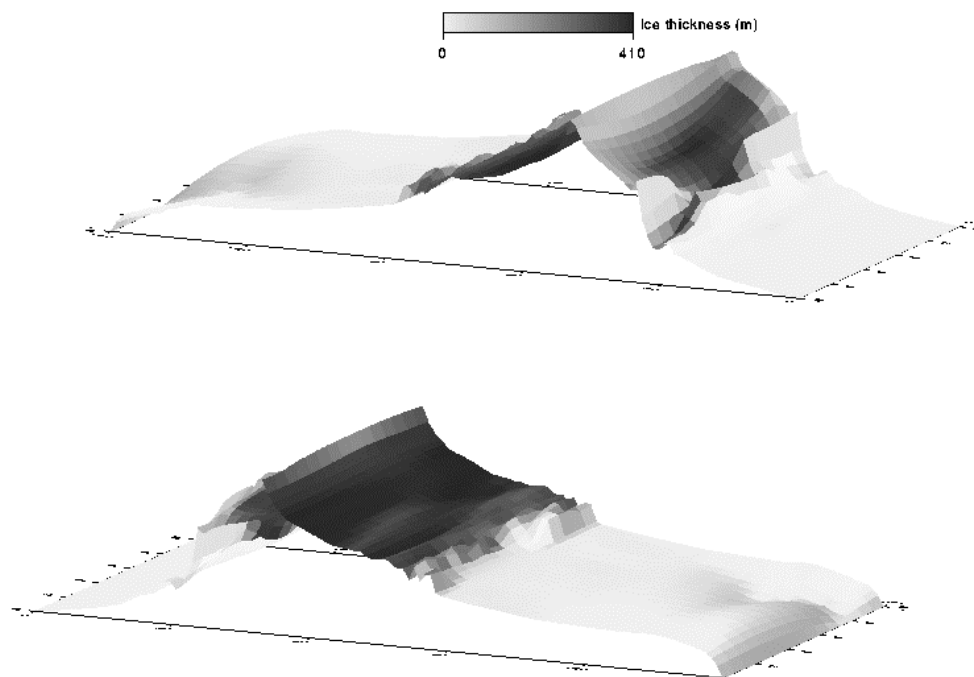


Figure 9: Two opposing views of the same simulated landscape. The shading represents ice thickness (the ice itself is not shown in the figure). Note the difference in topography between the ice covered and ice free regions.

Karst aquifer evolution in fractured, porous rocks

G. Kaufmann and J. Braun

The evolution of flow in a fractured, porous karst aquifer is studied by means of the finite element method on a two-dimensional mesh of irregularly spaced nodal points. Flow within the karst aquifer is driven by surface recharge from the entire region, simulating a precipitation pattern, and is directed towards an entrenched river as a base level. During the early phase of karstification, both the permeable rock matrix modeled as triangular elements and fractures within the rock matrix modeled as linear elements carry the flow. As the fractures are enlarged with time by chemical dissolution within the system calcite-carbon-dioxide-water, flow becomes more confined to the fractures. This selective enlargement of fractures increases the fracture conductivity by several orders of magnitude during the early phase of karstification. Thus, flow characteristics change from more homogeneous, pore-controlled flow to strongly heterogeneous, fracture-controlled flow.

Several scenarios for pure limestone aquifers, mixed sandstone-limestone aquifers are studied, and various surface recharge conditions as well as the effect of faulting on the aquifer evolution. Our results are sensitive to initial fracture width, faulting of the region, and recharge rate.

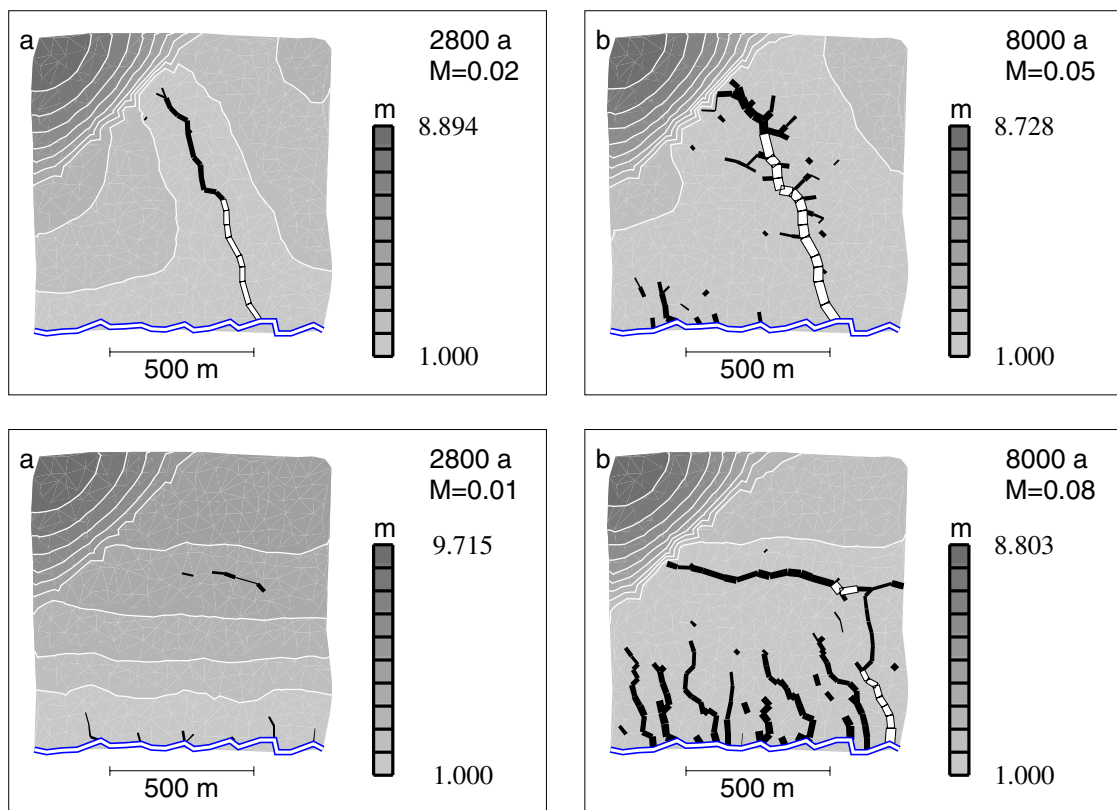


Figure 10: Enlargement of protoconduits in a sandstone-limestone aquifer by chemical dissolution. The hydrostatic head distribution in the aquifer is shown as greyscale image, with heads increasing from one meter along the base level (the double line representing a river) to around nine meter in the sandstone subdomain (top left corner). Enlarged fissures are shown as black boxes (laminar flow) or white boxes (turbulent flow). The initial protoconduits within the model domain have a diameter of 2 mm along a fault and 0.2 mm elsewhere. Shown are two time slices for an aquifer with a fault running from the sandstone subdomain to the river (top), and with a fault running approx. west-east and not connected to the base level (bottom).

